Spin-parity and broken symmetry in finite spin-$\frac{1}{2}$ chains with frustrated exchange: Quantum transition from high to low spin

Manoranjan Kumar and Zoltán G. Soos
Department of Chemistry, Princeton University, Princeton, New Jersey 08544, USA
(Received 24 January 2012; published 19 April 2012)

Exact diagonalization of finite spin-1/2 chains with periodic boundary conditions is applied to the ground state (GS) of chains with ferromagnetic (F) exchange $J_1 < 0$ between first neighbors, antiferromagnetic (AF) exchange $J_2 = \alpha J_1 > 0$ between second neighbors, and axial anisotropy $0 \leqslant \Delta \leqslant 1$. In zero field, the GS is in the $S_z = 0$ sector for the relevant parameters and is doubly degenerate at multiple points $\gamma_m = (\alpha_m, \Delta_m)$ in the α, Δ plane. Degeneracy under inversion at sites or spin-parity or both leads, respectively, to a bond order wave (BOW), to staggered magnetization, or to vector chiral (VC) order. Exact results up to $N = 28$ spins directly yield order parameters and spin correlation functions whose weak N dependencies allow inferences about infinite chains. The high-spin GS at $J_2 = 0$ changes discontinuously at $\gamma_1 = (-1/4, 1)$ to a singlet in the isotropic ($\Delta = 1$) chain. The transition from high to low spin $S(\alpha, \Delta)$ is continuous for $\Delta < \Delta_B = 0.95 \pm 0.01$ on the degeneracy line $\alpha_1(\Delta)$. The GS has staggered magnetization between $\Delta_A = 0.72$ and Δ_B and a BOW for $\Delta < \Delta_A$. When both inversion and spin-parity are reversed at γ_m, the correlation functions $C(p)$ for spins separated by p sites are identical. $C(p)$ minima are shifted by $\pi/2$ from the minima of VC order parameters at separation p, consistent with right- and left-handed helices along the z axis and spins in the xy plane. Degenerate GSs of finite chains are related to quantum phase diagrams of extended α, Δ chains, with good agreement for order parameters along the line $\alpha_1(\Delta)$. Degenerate GSs limit a VC phase to intermediate α and Δ where $S(\alpha, \Delta)$ varies rapidly but continuously, in contrast to many-body treatments in which VC phases extend over a larger range of parameters.

DOI: 10.1103/PhysRevB.85.144415 PACS number(s): 75.10.Jm, 75.10.Pq, 75.40.Cx, 05.30.Rt

I. INTRODUCTION

One-dimensional (1D) spin chains have been extensively studied over the years both experimentally and theoretically. Spin chains are good approximations to the magnetism of diverse inorganic and organic crystals. They are simple many-body quantum systems, well suited for computational studies,[1] with some exactly known properties and rich ground-state (GS) phase diagrams. Solid-state studies focus broadly on magnetic properties, instabilities, and phase transitions that limit 1D behavior at low temperature. Theoretical interest extends to quantum phases with different GSs in parameter space. In this paper we consider the GS properties of spin-1/2 chains [Eq. (1) below], with isotropic or axially anisotropic exchange J_1 between nearest neighbors and antiferromagnetic (AF) exchange $J_2 > 0$ between second neighbors that ensures frustration for either sign of J_1. The spin-Peierls system[2] $CuGeO_3$ illustrates spin-1/2 chains of Cu(II) ions with $J_1 > 0$. The isotropic AF/AF chain is a spin liquid up to[3] $\alpha = J_2/J_1 \leqslant 0.2411$, and its exact GS is a bond order wave (BOW) at $\alpha = 1/2$, the Majumdar-Ghosh point.[4]

Spin-1/2 Cu(II) chains with ferromagnetic (F) $J_1 < 0$ have recently been identified in cupric oxides[5–13] with estimated α ranging from[13] $\alpha \approx 0$ in $Ba_3Cu_3In_4O_{12}$ or $Ba_3Cu_3Sc_4O_{12}$ to[12,14] $\alpha \approx -0.5$ in $LiCuSbO_4$, $LiCuZrO_4$, $LiCuVO_4$, and $LiCu_2O_2$. The isotropic F/AF chain has a ferromagnetic GS for $\alpha = J_2/J_1 \geqslant \alpha_c = -1/4$, a singlet GS for $\alpha \leqslant \alpha_c$, and exact degeneracy at the quantum critical point α_c as shown by Hamada *et al.*[15] Vector chiral (VC) and multipolar phases have been of special interest.[14,16–20] Hikihara *et al.*[19] discuss the phase diagram of the isotropic F/AF chain in a static magnetic field. Furukawa *et al.*[17] and Sirker,[14] among others,[21] have studied the axially anisotropic F/AF chain in a zero field, the model considered in this paper. The limit $J_1 = 0$ decouples the system into two AF chains as sketched in Fig. 1 for a zigzag chain.

The Hamiltonian of the anisotropic F/AF chain with periodic boundary conditions (PBCs) and spin-1/2 sites is

$$H(\alpha, \Delta) = J_1 \sum_{p=1}^{N} (\vec{S}_p \cdot \vec{S}_{p+1} + \alpha \vec{S}_p \cdot \vec{S}_{p+2}) + (\Delta - 1)\left(S_p^z S_{p+1}^z + \alpha S_p^z S_{p+2}^z\right), \qquad (1)$$

where $J_1 = -1$ sets the energy scale. The model has two parameters, the frustration ratio $\alpha = J_2/J_1 < 0$ and axial anisotropy $0 \leqslant \Delta \leqslant 1$. Total spin S is conserved in the isotropic limit, $\Delta = 1$, but only S_z is a good quantum number otherwise. The GS is always in the $S_z = 0$ sector for the parameters of interest in this work, and $S_z = 0$ basis states are products of $N/2$ spins α and N/2 spins β. The GS transforms as $P = \pm 1$ under the spin-parity operator P that reverses all spins and as $C_i = \pm 1$ under inversion at sites, which corresponds to reflection through sites p, $p + N/2$ in finite systems. $H(\alpha, \Delta)$ also has C_N translational symmetry and inversion symmetry midway between sites.

The GS phase diagram of $H(\alpha, \Delta)$ has been studied by many-body methods[1,14,16–23] such a field theory, perturbation theory, and density matrix renormalization group (DMRG) that so far agree only in part. Broken symmetry is expected and found for ranges of α and Δ, with multiple exotic phases near the quantum critical point $\alpha_c = -1/4$, $\Delta = 1$. Excitation energies are small, of order $1/N$ for N spins and exceptionally small according to one field theory.[24] One challenge is to distinguish between strictly degenerate GSs that indicate broken symmetry and nondegenerate GSs with tiny excitation energies, as discussed carefully by Affleck and Lieb in 1D spin chains.[25]

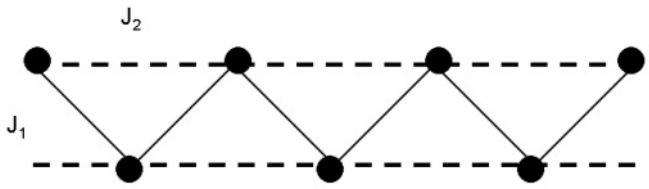

FIG. 1. Schematic representation of a spin-1/2 chain with exchange J_1 and J_2 between first and second neighbors.

We adopt a different approach that bears directly on broken symmetry and order parameters but only indirectly on the phase diagram. We solve $H(\alpha,\Delta)$ exactly for finite N up to $N = 28$. Since exact eigenstates respect all symmetries, broken symmetry requires degenerate GSs that in turn yield order parameters. On the other hand, phase boundaries from finite-size calculations are based on excited-state crossovers, or degeneracy, as discussed for the BOW phase of the isotropic AF/AF chain[3,26] or of extended Hubbard models.[27,28] Order parameters become nonzero at the boundary and increase in the broken-symmetry phase. As shown in Sec. II, $H(\alpha,\Delta)$ has a doubly degenerate GS at multiple parameter values $\gamma_m = (\alpha_m,\Delta_m), m = 1,2,\ldots,$ where the GS symmetry changes.

There are three kinds of GS degeneracy. When γ_m corresponds to $C_i = \pm 1$ or $P = \pm 1$, the linear combinations

$$|\gamma_m\rangle = (|\gamma_m,1\rangle \pm |\gamma_m,-1\rangle)/\sqrt{2} \tag{2}$$

have broken inversion or spin-parity symmetry and different order parameters. When both C_i and P are reversed at γ_m, either $(1,1)$ and $(-1,-1)$ or $(1,-1)$ and $(-1,1)$, the linear combinations in Eq. (2) have $C_i P = \pm 1$. There are finite-size gaps to all other eigenstates, sometimes remarkably small gaps. Broken C_i symmetry leads as usual to a BOW or dimer phase; broken parity P is associated with staggered magnetization or Néel order; broken C_i and P symmetry yields VC order. Dimer, Néel, and VC phases are all possibilities for $H(\alpha,\Delta)$ in a zero field.[14,17,19] Exact diagonalization, albeit limited to discrete γ_m, makes it possible to compute order parameters as well as spin correlations functions or other properties. When systematic variations with N are found, extrapolation gives accurate but not exact information about the infinite chain.

Increasing J_2 (increasing $-\alpha$) induces a quantum transition from a high to low spin. The isotropic chain has a first-order transition with discontinuous S at $\gamma_1 = (-1/4,1)$. S_z rather than S is conserved in systems with axial anisotropy $\Delta < 1$. The normalized spin per site $S(\alpha,\Delta)$ is the GS expectation value

$$2S(\alpha,\Delta) = \frac{2\langle\alpha,\Delta|S^2|\alpha,\Delta\rangle^{1/2}}{[N(N+2)]^{1/2}} \leqslant 1. \tag{3}$$

$S(\alpha,\Delta)$ is shown in Sec. III to be discontinuous for small anisotropy $\Delta > \Delta_B \approx 0.95$, continuous for $\Delta < \Delta_B$. There is finite Néel order between $\Delta_A = 0.75$ and Δ_B, finite BOW or dimer order for $\Delta < \Delta_A$. The spin transition requires exact GSs and has apparently not been recognized previously in anisotropic chains. Spin correlation function show spiral order at γ_m when C_i symmetry is broken, as in isotropic AF/AF chains.[26,29] We find identical spin correlations functions at parameter values γ_m when both C_i and P are broken, and interpret these results as right- and left-handed helices along the unique axis with spins in the xy plane. We compare finite-size results with previous theory and find considerable agreement as well as occasional disagreement. Our results limit VC degeneracy to small ranges of parameters α, Δ in which $S(\alpha,\Delta)$ varies rapidly but continuously. More extended VC phases have been inferred by other methods.[17,19]

II. DEGENERACY AND BROKEN SYMMETRY

We summarize some properties of the anisotropic F/AF spin chain [Eq. (1)] before presenting numerical results for even N with PBC. The GS is ferromagnetic at $J_2 = 0$ ($\alpha = 0$) with magnetization in the xy plane for $\Delta < 1$. Increasing $J_2 > 0$ (increasing $-\alpha$) induces a quantum transition to a low-spin state. The ferromagnetic and singlet GSs of the isotropic chain are degenerate at $\alpha_c = -1/4$ with energy per site $\epsilon_0 = -3/16$. The exact result for the extended system is the first degeneracy $\gamma_1 = (-1/4,1)$ for finite N, where S changes from $N/2$ to 0. Any singlet with $S_z = 0$ can be represented[30] as linear combinations of $N/2$ paired spins $(\alpha_i\beta_j - \beta_i\alpha_j)/\sqrt{2}$ whose phase is fixed by choosing site $i < j$. The parity is $P = (-1)^{N/2}$ since reversing all spins gives a phase factor of -1 for every singlet pair. The GS linear combination at α_c is the uniformly distributed resonating valence bond solid.[15]

The degeneracy $\gamma_1 = \alpha_1(\Delta)$ between high and low spin shifts to $\alpha_1(\Delta) < \alpha_c = -1/4$. The unit step function $2S(\alpha,1)$ at $\alpha_c = -1/4$ decreases rapidly for $\Delta < 1$, and $2S(\alpha,\Delta)$ is continuous for $\Delta < 0.95$. In the limit $\Delta = 0$ of extreme anisotropy, the crossover to low spin occurs at $\alpha_1(0) = -1/2$ for even N. The degeneracy $\gamma_1 = (-1/2,0)$ is the F/AF version of the Majumdar-Ghosh point of the isotropic AF/AF chain.[4] Here the exact GS is a product of triplets with $S_z = 0$, $(\alpha_i\beta_j + \alpha_i\beta_j)/\sqrt{2}$, with either $i = 2n-1$, $j = 2n$ or $i = 2n$, $j = 2n+1$. There are $N/2$ triplets, and Eq. (3) gives

$$S(-1/2,0) = 1/\sqrt{(N+2)}. \tag{4}$$

The exact result shows that the extended system has $S(\alpha,\Delta) = 0$ for $-\alpha \geqslant 1/2$ over the entire range of Δ. The singlet GS at $\Delta = 1$ becomes a linear combination of states with $S^2 \approx N$ in anisotropic chains, and the spin per site goes as $N^{-1/2}$ on the low-spin side.

Another relevant limit is $J_1 = 0$, when $H(\alpha,\Delta)$ decouples into chains with anisotropic $J_2 > 0$ between nearest neighbors as sketched in Fig. 1. $N = 4n$ systems decouple into 1D chains of $2n$ sites that correspond to the XXZ Heisenberg spin-1/2 antiferromagnet. The GS of each chain has $S_z = 0$, and there are no correlations between spins in different chains. On the other hand, $N = 4n+2$ systems decouple into two radicals with $S_z = \pm 1/2$ whose GSs remain entangled even at $J_1 = 0$. We find $4n$, $4n+2$ effects in isotropic chains around $\alpha \approx -1/2$, but none at $\gamma_1 = \alpha_1(\Delta)$.

We obtain the lowest energy of $H(\alpha,\Delta)$ [Eq. (1)] for even N and PBC in four sectors with $S_z = 0$, $C_i = \pm 1$, and $P = \pm 1$. The absolute GS is degenerate at points $\gamma_m = (\alpha_m,\Delta_m)$ that are found to two or three significant figures. Preliminary scans for small N on a rougher grid identifies parameter ranges with symmetry crossovers. Figure 2 shows the γ_m in the $-\alpha$, Δ plane for $N = 20$. Open circles indicate C_i degeneracy, closed circles P degeneracy, and stars VC degeneracy. The points α_1 at $\Delta = 1$ and 0 are exact, independent of size, and the line $\gamma_1 =$

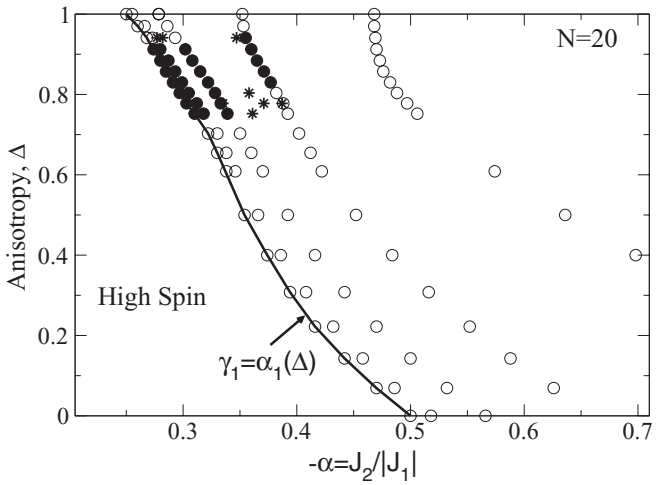

FIG. 2. Parameter points (α,Δ) for a doubly degenerate GS of $H(\alpha,\Delta)$ [Eq. (1)] with $N = 20$ spins. Open circles indicate inversion degeneracy $C_i = \pm 1$, closed circles indicate spin-parity degeneracy $P = \pm 1$, and stars indicate vector chiral degeneracy $C_i P = \pm 1$. The line $\alpha_1(\Delta)$ marks degeneracy between high and low spin.

$\alpha_1(\Delta)$ hardly depends on N. All degeneracy for $\Delta < 0.7$ is associated with inversion symmetry. Staggered magnetization or VC order is limited to intermediate anisotropy in Fig. 2. The intermediate region is expanded in Fig. 3 for $N = 24$.

Table I lists the $n-1$ values of $(-\alpha_m,1)$, $m \geqslant 2$, for isotropic $N = 4n$ chains, all with $C_i = \pm 1$. Anisotropic $N = 4n$ chains with $\Delta < 0.7$ also have n degenerate points α_m with $C_i = \pm 1$. Broken-symmetry GSs are given by Eq. (2). When γ_m corresponds to $C_i = \pm 1$, the BOW or dimer amplitude $B(\gamma_m)$ is

$$B(\gamma_m) = \langle \gamma_m; -1|(S_1 \cdot S_2 - S_2 \cdot S_3)|\gamma_m; 1\rangle/2. \qquad (5)$$

The order parameter is the off-diagonal matrix element, $\pm B$ for the two GSs, and we used translational symmetry. Only BOWs are realized in isotropic $(\Delta = 1)$ systems whose $B(\alpha_m,1)$ are shown in Fig. 4 for both $N = 4n$ and $4n+2$. $B(\alpha,1)$ has a broad maximum around $\alpha \approx -0.5$ and a modest size dependence. DMRG results in Fig. 4 are based on an

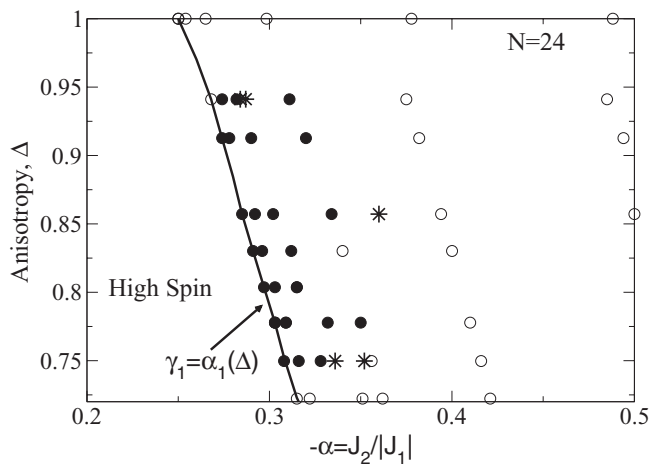

FIG. 3. Same as Fig. 2 for $N = 24$ at intermediate anisotropy Δ and frustration α.

TABLE I. Degenerate ground states at $(-\alpha_m,1)$, $m \geqslant 2$, of isotropic spin chains [Eq. (1)] with N sites and $\Delta = 1$.

N	$-\alpha_2$	$-\alpha_3$	$-\alpha_4$	$-\alpha_5$	$-\alpha_6$	$-\alpha_7$
8	0.342					
12	0.276	0.401				
16	0.260	0.318	0.439			
20	0.254	0.279	0.352	0.467		
24	0.254	0.265	0.299	0.378	0.488	
28	0.251	0.259	0.288	0.338	0.381	0.510

algorithm[31] that adds four spins per step, as needed for accuracy at $-\alpha > 0.5$, and gives fragments with an even number of sites at each step. The AF/AF chain has a broad maximum[28] $B(0.4,1) = 0.40$ that is 10-fold larger. The z and transverse parts of $B(\alpha_m)$ are found separately in anisotropic systems with $\Delta < 1$. Most γ_m in Figs. 2 and 3 refer to degeneracy under inversion, and $B(-1/2,0) = 1/8$ is exact.

When γ_m corresponds to $P = \pm 1$, the amplitude $M_{\rm st}(\gamma_m) > 0$ of the staggered magnetization is

$$M_{\rm st}(\gamma_m) = \tfrac{1}{2}\langle \gamma_m; -1|\left(S_1^z - S_2^z\right)|\gamma_m; 1|\rangle. \qquad (6)$$

Similarly, when both C_i and P are reversed at γ_m, the VC order parameters $\pm\kappa_z(p;\gamma_m)$ for spins p sites apart are

$$\kappa_z(p,\gamma_m) = \langle \gamma_m; -1, -1|(\vec{S}_1 \times \vec{S}_{1+p})_z|\gamma_m; 1,1\rangle$$
$$= \frac{i}{2}\langle \gamma_m; -1, -1|(S_1^+ S_{1+p}^- - S_1^- S_{1+p}^+)|\gamma_m; 1,1\rangle. \qquad (7)$$

The z component of the vector product is finite for axial anisotropy, and Eq. (7) is for degeneracy between (1,1) and $(-1,-1)$. The matrix element has $(-1,1)$ and $(1,-1)$ for the other way of reversing both C_i and P. We paid close attention to degenerate points γ_m and found only twofold degeneracy. In a few cases, the gap to the first excited state is tiny, of the order of 10^{-5}, far less than $1/N$. Double degeneracy implies one broken symmetry in finite chains for any (α,Δ) in the range $-\alpha > 1/4$, $0 \leqslant \Delta \leqslant 1$.

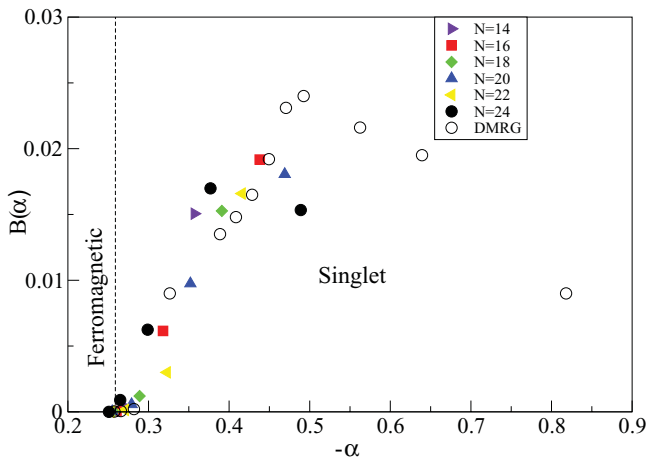

FIG. 4. (Color online) Discrete order parameter $B(\alpha_m)$ [Eq. (5)] as a function of frustration α in isotropic $(\Delta = 1)$ chains of N sites; continuous $B(\alpha)$ from DMRG.

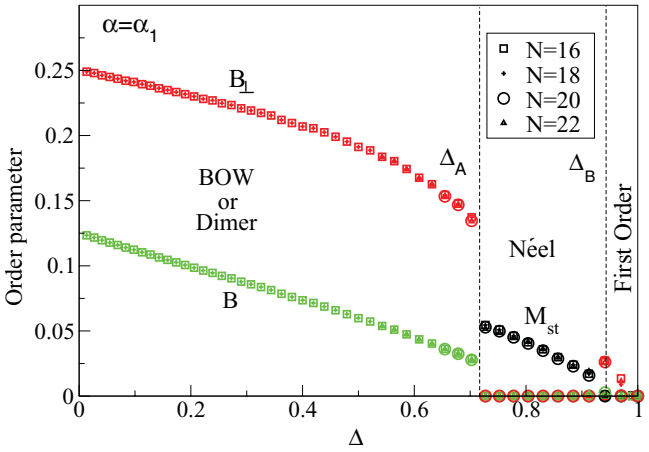

FIG. 5. (Color online) Order parameters along the degeneracy line $\alpha_1(\Delta)$ between high and low spin. B and $B_\perp$ are Eq. (5) and its transverse part, and M_{st} is Eq. (6). The spin transition of the infinite chain is first order for $\Delta \geqslant \Delta_B$ and has vanishing order parameters.

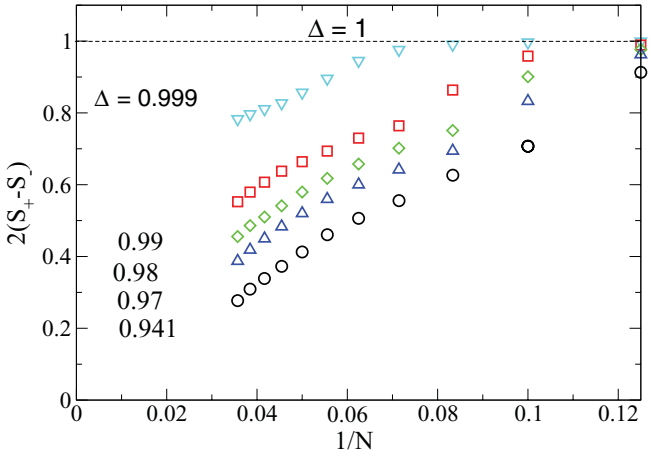

FIG. 6. (Color online) Discontinuity in $S(\alpha,\Delta)$ [Eq. (3)] at the degeneracy $\alpha_1(\Delta)$ between high and low spin in system of N spins with axial anisotropy Δ up to $N = 28$.

The order parameters $B(\gamma_1)$, its transverse part $B_\perp$, and $M_{st}(\gamma_1)$ are shown in Fig. 5 as a function of anisotropy along $\gamma_1 = \alpha_1(\Delta)$. The size dependence is negligible, and $\Delta = 0$ is exact, with $B = 1/8$, $B_\perp = 1/4$. As mentioned above, finite $B(\gamma_1)$ or $M_{st}(\gamma_1)$ implies that the phase boundary where the order parameter becomes nonzero is on the high-spin side of γ_1, but deviations from γ_1 are significant only for large order parameters. The largest difference occurs at $\Delta = 0$, where $\alpha_1 = -0.50$ and excited-state crossovers give $\alpha = -0.325$. The dimer/Néel boundary in Fig. 5 is $\Delta_A(N) = 0.722$ with $\alpha_A = -0.317$ for $N = 18$, 20, and 22, while the Néel/first-order boundary is $\Delta_B(N) = 0.941$ with $\alpha_B = -0.2674$. The staggered magnetization increases with anisotropy in the Néel phase to 0.050 at Δ_A. $B(\alpha_1)$ is small (<0.03) and decreases with N near Δ_B in the first-order region where we expect $B = 0$ in the extended system. For comparison, the infinite time-evolving block decimation (iTEBD) algorithm[17] gives $\Delta_A = 0.72$, $\alpha_A = -0.320$ and $\Delta_B = 0.93$, $\alpha_B = -0.272$ in Fig. 4 of Ref. 17(a); the maximum Néel amplitude is 0.055 and $2B_\perp$ (called D^{xy}_{123}) $= 0.35$ at $\Delta = 0.65$ where we find $2B_\perp = 0.309$ at $N = 16$ and 0.307 at $N = 22$. There is remarkably close agreement between two completely different calculations. We disagree near $\Delta = 1$ where iTEBD returns small finite B rather than $B = 0$.

III. SPIN TRANSITION AND CORRELATION FUNCTIONS

We evaluate the spin per site $2S(\alpha,\Delta)$ [Eq. (3)] for slightly anisotropic systems along the degeneracy $\gamma_1 = \alpha_1(\Delta)$ between high (S_+) and low spin (S_-). The size dependence of $S_+(\Delta) - S_-(\Delta)$ is shown in Fig. 6 up to $N = 28$. The step function of isotropic chains is quickly lost with increasing N. Although $1/N$ behavior is approximate at best, the gap has vanished by $\Delta = 0.94$, and the extended system has a continuous transition for $\Delta < \Delta_B = 0.95 \pm 0.01$. The $S(\alpha,\Delta)$ discontinuity at $\alpha_1(\Delta)$ clearly decreases very rapidly with anisotropy. The precise value of Δ_B is less important than recognizing a first-order quantum transition for $\Delta > \Delta_B$. Orthogonality in S then ensures vanishing order parameters for an infinite chain with a first-order transition in Fig. 5. As an indication of internal consistency, we note that almost identical values of Δ_B are inferred from closing the $S_+(\Delta) - S_-(\Delta)$ discontinuity and from the Néel/first-order boundary.

We define GS correlation functions for spins p sites apart using the translational symmetry of $H(\alpha,\Delta)$

$$C(p,\gamma) = \langle\gamma|(\vec{S}_1 \cdot \vec{S}_{1+p})|\gamma|\rangle = C_z(p,\gamma) + C_\perp(p,\gamma). \quad (8)$$

The z and transverse components are computed separately and are not simply related in anisotropic systems. For $S = 1/2$ chains, we have

$$\langle\gamma|S^2_z|\gamma\rangle/N = \frac{1}{4} + \sum_{p=1}^{N-1} C_z(p,\gamma),$$
$$\langle\gamma|S^2_\perp|\gamma\rangle/N = \frac{1}{2} + \sum_{p=1}^{N-1} C_\perp(p,\gamma). \quad (9)$$

Since the GS is in the $S_z = 0$ sector, finite $S(\alpha,\Delta)$ is due to transverse components. The high-spin regime with $-\gamma \leqslant \alpha_1(\Delta)$ has $C(p) > 0$ for all p, or simply $C(p) = 1/4$ at $\Delta = 1$. The low-spin regime necessarily has $C(p) < 0$ for some p, and PBC implies an even number of sign changes as a function of p.

The upper panel of Fig. 7 shows $C(p,\alpha_2)$ in isotropic chains up to $N = 28$ as a function of $\theta = 2\pi p/N$ with $p = 1,2,\ldots,N-1$. At $\Delta = 1$, there are two sign changes in the interval $[-1/4,\alpha_2]$ and four sign changes in $[\alpha_2,\alpha_3]$. $C(p,\alpha_2)$ is double valued. The systematic size dependence allows inferences about the extended system. The line in Fig. 7(a) has small deviations from sinusoidal due to $C(0) = 3/4$, whose contribution decreases as $1/N$. $C(p,\gamma)$ changes sign $2n$ times for $-\gamma > \gamma_n$, as shown in Fig. 7 for $N = 20$, lower panel, for isotropic chains at $\gamma_5 = \alpha_5(1)$. For comparison, we include the limit $J_1 = 0$, when $C(p) = 0$ for odd p and has alternating sign for even p. The $J_1 = 0$ calculation is for a longer chain that shows decreasing AF correlation with increasing p. Although $\alpha_n(1) \approx -1/2$ in Table I is far from the $J_1 = 0$

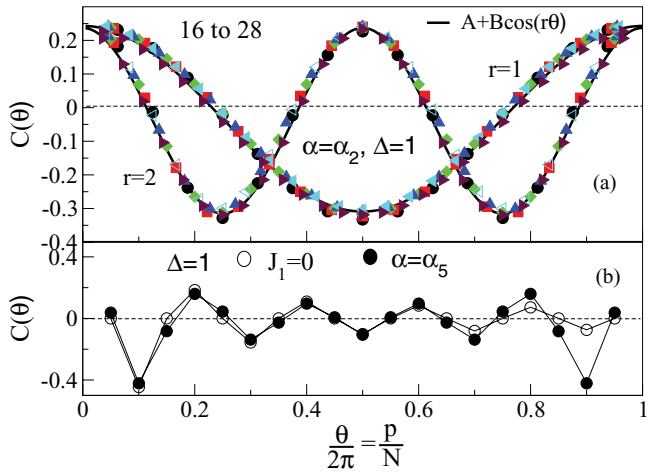

FIG. 7. (Color online) Spin correlation functions $C(\theta)$ [Eq. (8)] with $\theta = 2\pi p/N$, of isotropic chains $H(\alpha,1)$ [Eq. (1)]. Upper panel: α_2 up to $N = 28$ with $2r$ changes of sign; the $r = 1$ and 2 lines have $B = 0.276$, $A = -0.0426$. Lower panel: Closed symbols, α_5 for $N = 20$ with 10 sign changes; open symbols, decoupled chains with $J_1 = 0$ and $C(p) = 0$ for odd p.

limit ($\alpha \to -\infty$) of decoupled AF chains, the spin correlation functions are already similar. They change sign at most $2n$ times and account fully for the GS degeneracy of isotropic $N = 4n$ chains. Isotropic chains, either F/AF or AF/AF, are limited to BOW or dimer phases, in clear disagreement with the VC phase in zero field in Fig. 1(a) of Ref. 19 or, in a smaller range, in Fig. 2(b) of Ref. 17(b).

$C(p;\gamma_m)$ of anisotropic chains are not sinusoidal but still have $2m-2$ and $2m$ sign changes when γ_m marks broken C_i or P symmetry. The $C(p,\gamma_2)$ in Fig. 8 are for Néel order and $N = 24$. There are two and four sign changes as expected. $N = 4n$ chains have n points γ_m with broken C_i or P symmetry. Additional degeneracy, if any, is exclusively due to the broken C_i and P symmetry that indicates VC order. Returning to Figs. 2 and 3, we see that lines $\gamma_m = \alpha_m(\Delta)$ through the mth degeneracy, either C_i or P, of finite systems partition parameter space into regions in which $C(p)$ changes sign $2m-2$ and $2m$ times.

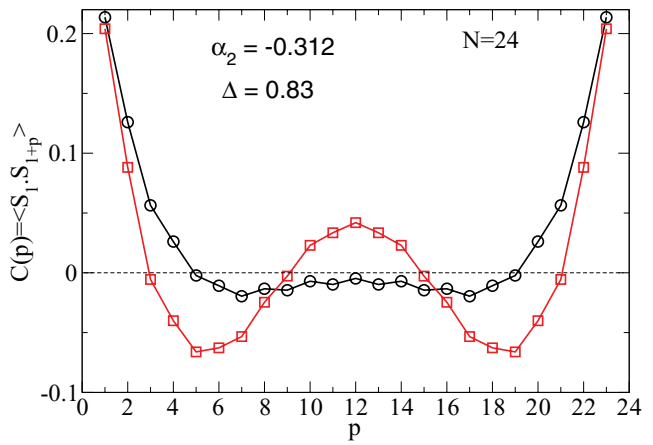

FIG. 8. (Color online) Spin correlation functions $C(p)$ of a 24-site chain with spin-parity degeneracy at $\alpha_2 = -0.312$, $\Delta = 0.83$.

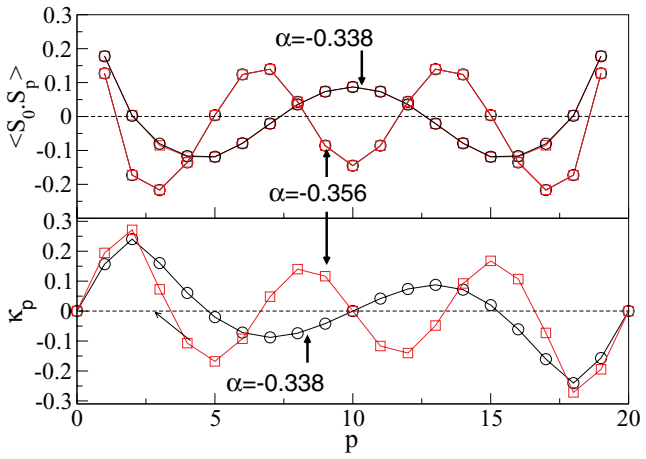

FIG. 9. (Color online) Spin correlation functions $C(p)$ and order parameters $\kappa_z(p)$ [Eq. (7)] of a 20-site chain with VC degeneracies at $\Delta = 0.75$ and $\alpha = -0.338$ and -0.357.

The GS energy per site, $\epsilon_0(\alpha,\Delta)$, is related to spin correlation functions of first and second neighbors

$$\epsilon_0(\alpha,\Delta) = -C_\perp(1) - \Delta C_z(1) + \alpha C_\perp(2) + \alpha\Delta C_z(2). \quad (10)$$

Degenerate $\epsilon_0(\alpha,\Delta)$ at $\gamma_m = \alpha_m(\Delta)$ is achieved with unequal $C(1;\gamma_m), C(2;\gamma_m)$ in Figs. 7 and 8. Finite-size effects generate small discontinuities in $S(\alpha,\Delta)$ at all γ_m with unequal $C(p;\gamma_m)$. It is straightforward to count the number of C_i or P degeneracies in finite systems. We cannot predict the number of VC degeneracy, the stars in Fig. 2 and 3, and a finer grid may reveal additional GS degeneracy leading to VC order.

In contrast to P or C_i degeneracy, degenerate $\epsilon_0(\alpha,\Delta)$ under reversal of both C_i and P lead to *equal* spin correlation functions as shown in Fig. 9, upper panel, for $N = 20$, $\Delta = 0.75$, $\alpha = -0.338$ and -0.356. The first point has four sign changes, in accord with two P degeneracies at smaller $-\alpha$. There is a C_i degeneracy between the two VC points, which accounts for six sign changes at $-\alpha = 0.356$. We always find equal $C(p;\gamma_m)$ at VC degeneracies within our 3–4 digit numerical accuracy, except for $N = 4n+2$ systems with $-\alpha > 0.5$, where equality is limited to two digits and there are pronounced $4n$, $4n+2$ effects. Equal $C(p;\gamma_m)$ for all p implies equal $S(\gamma_m)$ according to Eq. (9). The VC order parameters $\kappa_z(p;\gamma_m)$ [Eq. (6)]) in the lower panel of Fig. 9 has the same periodicity, but they vanish at points that are shifted by $\pi/2$. It follows from Eqs. (7) and (8) that when γ_m refers to VC degeneracy:

$$\langle S_1^+ S_{1+p}^- \rangle = -C_\perp(p,\gamma_m) - i\kappa_z(p,\gamma_m). \quad (11)$$

VC order parameters are closely related to transverse spin correlation functions in chains with axial anisotropy.

A simple classical picture captures the principal features of quantum spins with VC order $\pm\kappa_z(p)$. Right- and left-handed helices are doubly degeneracy with equal energy $\epsilon_0(\gamma_m)$ and spin $S(\gamma_m)$. $H(\alpha,\Delta)$ has axial symmetry in spin space and spins in the xy plane for $\Delta < 1$. We picture the two helices as $(x_n, \pm y_n) = (\cos n\phi, \pm \sin n\phi)$ with pitch angle ϕ that generates a specified number of sign changes between $n = 1$ and N. Inversion gives $n \to -n$ and interchanges the helices.

Spin parity reverses the z and y components of spin, but not $s_x = (s^+ + s^-)/2$, and also interchanges the helices. Equal $C(p,\gamma_m)$ follow from projecting the helices on a plane that includes the z axis, as illustrated by $2\langle x_n x_{n+p}\rangle_n = 2\langle y_n y_{n+p}\rangle_n = \cos p\phi$ where $\langle\cdots\rangle_n$ indicates an average over n. The VC order parameters $\kappa_z(p,\gamma_m)$ go as $\pm 2\langle x_n y_{n+p}\rangle_n = \pm\sin p\phi$, shifted by $\pi/2$.

When $H(\alpha,\Delta)$ in Eq. (1) has classical spins, the GS is easily shown by energy minimization to be a spiral with pitch angle φ that depends only on α:

$$\cos\varphi = -J_1/4J_2 = -1/4\alpha. \tag{12}$$

A finite chain with PBC has $N\varphi = 2\pi m$. The critical point $-4\alpha = 1$ corresponds to $\varphi = 0$, the ferromagnetic GS. Finite $N = 4n$ limits the remaining angles to $n-1$ values $0 < \varphi < \pi/2$. Spiral spin correlation functions appear automatically in DMRG treatments[29,31] of isotropic spin-1/2 AF/AF chains. This follows directly from a singlet GS and Eq. (8) with $2C_z(p) = C_\perp(p)$, although DMRG is not accurate for the sum over all spin correlation functions. A spiral interpretation of $C(p,\gamma_m)$ holds in finite F/AF chains at any γ_m or, indeed, at any (α,Δ). There are crucial differences, however, between helices and spirals. Left- and right-handed helices are degenerate at γ_m with reversed C_i and P symmetry. Spirals are associated with $C_i = \pm 1$ and BOW phases but are not degenerate in $\pm\varphi$ in Eq. (12). The pitch angle $\varphi = \phi$ of spiral or helices of classical spins follows immediately from PBC. Table I lists degenerate γ_m at $\Delta = 1$ for quantum spins that can be converted to angles φ_m using Eq. (12). The proper number of γ_m is found for each N, but the actual values differ considerably for $-\alpha > 0.4$. Moreover, the points $\gamma_m = \alpha_m(\Delta)$ vary substantially with anisotropy.

IV. DISCUSSION

Quite unusually for model Hamiltonians, finite spin-1/2 chains with $H(\alpha,\Delta)$ in Eq. (1), periodic boundary conditions, and frustrated exchanges $J_1 < 0$ and $J_2 = \alpha J_1 > 0$ have a doubly degenerate ground state (GS) at many parameter values $\gamma_m = (\alpha_m, \Delta_m)$. There are three kinds of GS degeneracy: inversion symmetry $C_i = \pm 1$ or spin-parity $P = \pm 1$ or reversal of both C_i and P. We have exploited degeneracy for finite N using exact diagonalization to construct broken-symmetry GSs according to Eq. (2). Exact GSs make it possible to compute order parameters for broken symmetry, spin correlation functions $C(p,\gamma_m)$ in Eq. (8), and the normalized expectation value $S(\alpha,\Delta)$ of the total spin in Eq. (3). Access to exact GS properties compensates to some extent for the inherent limitations of finite-size approaches to infinite chains.

We have focused on GS degeneracy to construct and characterized broken-symmetry states. The quantum phase diagram derived from finite systems invoke excited-state degeneracy.[3,27] Our finite-size results are summarized in Fig. 10. The indicated phase boundary is based on the excited-state degeneracy between first excited state in $S_z = 0$ and the $S_z = \pm 1$ GS up to $N = 28$, as discussed in related 1D systems[2,27–29] that conserve S. The N dependence of the excited-state degeneracy is comparably weak and independent of Δ. The order parameter becomes nonzero and an energy gap opens very slowly[3,28] at a Kosterlitz-Thouless transition.

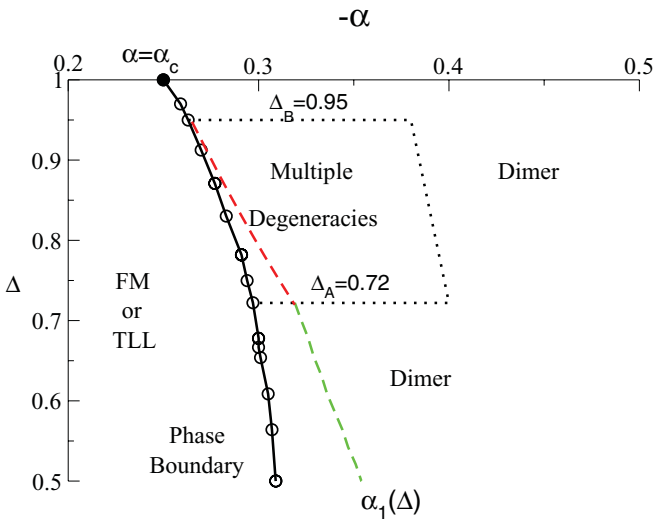

FIG. 10. (Color online) Approximate GS phase diagram of the anisotropic F/AF chain $H(\alpha,\Delta)$ [Eq. (1)]. The phase boundary between high and low spin is an excited-state crossover discussed in the text. The degeneracy line $\alpha_1(\Delta)$ has Néel order between Δ_A and Δ_B, dimer order for $\Delta < \Delta_A$. Dashed lines enclose regions with multiple degeneracies (inversion, spin-parity, both) where phases are not assigned.

The high-spin phase[17] is a ferromagnet or a Tomonaga-Luttinger liquid (TLL). We find the transition between high and low spin to be first order for $\Delta_B > 0.95$, continuous for $\Delta < \Delta_B$. Degeneracy along $\gamma_1 = \alpha_1(\Delta)$ is exact at $\Delta = 1$ or 0 and depends very weakly on N in between; as seen in Fig. 5, there is Néel order along along the line between Δ_A and Δ_B, dimer or BOW order for $\Delta < \Delta_A$. An almost identical boundary is shown in Fig. 4 of Ref. 17(a) or Fig. 2(b) of Ref. 17(b), based on $\alpha = J_2/|J_1|$ as a perturbation to an exact field theory at $\Delta = 0$. As noted in connection with Fig. 5, the order parameters of the dimer and Néel phases also agree well.

Multiple degeneracy is limited to intermediate anisotropy Δ and frustration ratio α close to $\alpha_1(\Delta)$. The dashed lines in Fig. 10 enclose the parameter space in which we find all three kinds of GS degeneracy. We cannot assign phases in this region. The degeneracies in Figs. 2 and 3 do not evolve systematically with N. Finite-size results merely place restrictions on phase boundaries. The isotropic ($\Delta = 1$) chain is limited to a BOW or dimer phase for $-\alpha < 1/4$, consistent with exclusively C_i degeneracy in Table I.

Broken C_i symmetry leading to a dimer or BOW phase dominates on the low-spin side. We find $B_z(\gamma_m)$, the z part of the order parameter in Eq. (5), to change sign with decreasing Δ, from singlet-type pairing at $\Delta = 1$ where the GS is a singlet to triplet-type pairing that is exact at $\Delta = 0, \alpha = -1/2$. A dimer triplet phase appears for small Δ in Fig. 2(b) of Ref. 17(b), separated by a VC phase from a dimer singlet phase. We do not find evidence for VC order outside the dashed lines in Fig. 10 and consider the sign of $B_z(\gamma_m)$ to be incidental in the dimer phase. The small region of multiple degeneracies in Fig. 10 is the major difference with the extensive VC regions in some[17,19,20,22] zero-field phase diagrams, but not in others.[14,23]

Finite-size results complement approximate treatment of extended systems. DMRG grows a discrete extended chain, while field theory deals with a continuum version of the chain. DMRG[29,31] results for F/AF or for AF/AF spin-1/2 chains are for open boundary conditions and even N that increases by two or four sites per step. Even chains have inversion symmetry at the center of the middle bond, but not C_i at any site, and C_i is relevant for GS degeneracy. Exact treatment of a half-filled band of N free electrons with open boundary conidtions leads to a nondegenerate GS[28,31] with a BOW whose amplitude B decreases as $1/N$ and excitation energies of order $1/N$. DMRG works well for model parameters leading to substantial $B > 0.01$ such as the broad peak around $\alpha \approx -0.4$ for isotropic F/AF chains in Fig. 4. But DMRG fails in extended 1D systems where, as discussed by Affleck and Lieb,[25] the distinction between GS degeneracy and $1/N$ excitation energies has to be considered.

Turning to field theory, we note that a continuum model is an approximation, that additional approximations are typically needed, and that different field theories are possible for $H(\alpha,\Delta)$. Two field theories[24,29] for isotropic AF/AF chains are not limited to $J_1 > 0$. The anisotropic F/AF chain has been treated with first-order corrections in J_2/J_1 starting[17] with exact field theory at $J_2 = 0$ and also as bosonization[19] in the opposite limit of $|J_1| \ll J_2$. The merits of field theory are beyond the scope of this paper. A continuum models suppresses the important distinction between inversion symmetry at sites and at the centers of bonds.

We have discussed frustrated chains with axial anisotropy for parameters leading to GSs in the $S_z = 0$ sector. The energy spectrum of isotropic ($\Delta = 1$) chains in a magnetic field $h = g\mu_B H$ that defines the z axis is simply the zero-field energy plus the Zeeman energy hm, with $m = \pm 1, \pm 2, \ldots, \pm S$ for states with spin S. The system has axial symmetry for $h > 0$, but spin-parity is no longer conserved. In strong fields, the GS has multipolar phases near the boundary between high and low spin.[19] The general problem of $H(\alpha,\Delta)$ plus a static field is considerably more complicated because S_z is conserved only when h is along the unique axis. Otherwise, the GS has to be found by separately as a function of h.

In summary, finite F/AF models $H(\alpha,\Delta)$ [Eq. (1)] with frustration ratio $\alpha = J_2/J_1$ and axial anisotropy $0 \leqslant \Delta \leqslant 1$ have a doubly degenerate GS at multiple points $\gamma_m = (\alpha_m, \Delta_m)$, all in the $S_z = 0$ sector. Exact GSs make it possible to compute order parameters at γ_m, spin correlation functions and the spin per site, $S(\alpha,\Delta)$. The transition from high to low spin with increasing $-\alpha$ is first order for $\Delta > 0.95$, continuous for $\Delta < 0.95$, with staggered magnetization or Néel order for $0.72 < \Delta < 0.95$ and dimer order for stronger anisotropy $\Delta < 0.72$. When both C_i and P symmetry are broken, VC order leads to identical spin correlation functions and $S(\alpha,\Delta)$ that is interpreted as right- and left-handed helices along the unique axis with spins in the xy plane. Finite-size effects are typically quite small, small enough to discuss infinite chains. Exact finite-size results are consistent with with many-body treatments aside from limiting a possible VC phase to intermediate α and Δ where $S(\alpha,\Delta)$ varies rapidly but continuously.

ACKNOWLEDGMENTS

We thank S. Dutton and R. Cava for stimulating discussions of frustrated Cu(II) chains. This work was largely performed at the TIGRESS high-performance computer center at Princeton University, which is jointly supported by the Princeton Institute for Computational Science and Engineering and the Princeton University Office of Information Technology. We thank the National Science Foundation for partial support of this work through the Princeton MRSEC (DMR-0819860).

[1] A. W. Sandvik, AIP Conf. Proc. **1297**, 135 (2010) and references therein.
[2] M. Hase, I. Terasaki, and K. Uchinokura, Phys. Rev. Lett. **70**, 3651 (1993).
[3] K. Okamoto and K. Namura, Phys. Lett. A **169**, 433 (1992).
[4] C. K. Majumdar and D. K. Ghosh, J. Math. Phys. **10**, 1399 (1969).
[5] M. Hase, H. Kuroe, K. Ozawa, O. Suzuki, H. Kitazawa, G. Kido, and T. Sekine, Phys. Rev. B **70**, 104426 (2004).
[6] H. T. Lu, Y. J. Wang, S. Qin, and T. Xiang, Phys. Rev. B **74**, 134425 (2006).
[7] T. Masuda, A. Zheludev, A. Bush, M. Markina, and A. Vasiliev, Phys. Rev. Lett. **92**, 177201 (2004); S. Zvyagin, G. Cao, Y. Xin, S. McCall, T. Caldwell, W. Moulton, L.-C. Brunel, A. Angerhofer, and J. E. Crow, Phys. Rev. B **66**, 064424 (2002).
[8] Y. Mizuno, T. Tohyama, S. Maekawa, T. Osafune, N. Motoyama, H. Eisaki, and S. Uchida, Phys. Rev. B **57**, 5326 (1998).
[9] G. Kamieniarz, M. Bielinski, G. Szukowski, R. Szymczak, S. Dyeyev, and J.-P. Renard, Comput. Phys. Commun. **147**, 716 (2002).
[10] S.-L. Drechsler, O. Volkova, A. N. Vasiliev, N. Tristan, J. Richter, M. Schmitt, H. Rosner, J. Málek, R. Klingeler, A. A. Zvyagin, and B. Büchner, Phys. Rev. Lett. **98**, 077202 (2007).
[11] O. S. Volkova, I. S. Maslova, R. Klingeler, M. Abdel-Hafiez, A. U. B. Wolter, B. Büchner, and A. N. Vasiliev, e-print arXiv:1111.1186.
[12] S. E. Dutton, M. Kumar, M. Mourigal, Z. G. Soos, J.-J. Wen, C. L. Broholm, N. H. Andersen, Q. Huang, M. Zbiri, R. Toft-Petersen, R. J. Cava, Phys. Rev. Lett. (in press), e-print arXiv:1109.4061.
[13] S. E. Dutton, M. Kumar, J. Crawford, Z. G. Soos, C. L. Broholm, and R. J. Cava, J. Phys.: Condens. Matter **24**, 166001 (2012).
[14] J. Sirker, Phys. Rev. B **81**, 014419 (2010).
[15] T. Hamada, J. Kane, S. Nakagawa, and Y. Natusume, J. Phys. Soc. Jpn. **57**, 1891 (1988).
[16] S. W. Cheong and M. Mostovoy, Nat. Mater. **6**, 13 (2007).
[17] S. Furukawa, M. Sato, and A. Furusaki, Phys. Rev. B **81**, 094430 (2010); S. Furukawa, M. Sato, and S. Onoda, Phys. Rev. Lett. **105**, 257205 (2010).
[18] D. V. Dmitriev and V. Ya. Krivnov, Phys. Rev. B **77**, 024401 (2008).
[19] T. Hikihara, L. Kecke, T. Momoi, and A. Furusaki, Phys. Rev. B **78**, 144404 (2008).

[20]J. Sudan, A. Lüscher, and A. M. Laüchli, Phys. Rev. B **80**, 140402(R) (2009).
[21]S. Mahdavifar, J. Phys.: Condens. Matter **20**, 335230 (2008).
[22]F. Heidrich-Meisner, I. P. McCulloch, and A. K. Kolezhuk, Phys. Rev. B **80**, 144417 (2009).
[23]T. Hikihara, T. Momoi, A. Furusaki, and H. Kawamura, Phys. Rev. B **81**, 224433 (2010).
[24]C. Itoi and S. Qin, Phys. Rev. B **63**, 224423 (2001).
[25]I. Affleck and E. H. Lieb, Lett. Math. Phys. **12**, 57 (1986).
[26]M. Kumar, S. Ramasesha, and Z. G. Soos, Phys. Rev. B **81**, 054413 (2010).
[27]M. Nakamura, Phys. Rev. B **61**, 16377 (2000); J. Phys. Soc. Jpn. **68**, 3123 (1999).
[28]M. Kumar, S. Ramasesha, and Z. G. Soos, Phys. Rev. B **79**, 035102 (2009).
[29]S. R. White and I. Affleck, Phys. Rev. B **54**, 9862 (1996).
[30]S. Ramasesha and Z. G. Soos, in *Theoretical and Computational Chemistry*, Vol. 10, edited by D. L. Cooper (Elsevier, Amsterdam, 2002), p. 635; Z. G. Soos and S. Ramasesha, Phys. Rev. B **29**, 5410 (1984); S. Ramasesha and Z. G. Soos, Int. J. Quantum Chem. **25**, 1003 (1984); Z. G. Soos and S. Ramasesha, in *Valence Bond Theory and Chemical Structure*, edited by D. J. Klein and N. Trinajstic (Elsevier, Amsterdam, 1989), p. 81.
[31]M. Kumar, Z. G. Soos, D. Sen, and S. Ramasesha, Phys. Rev. B **81**, 104406 (2010).